applied sciences

Communication

Wavelength Conversion of Multi-Joule Energy 532 nm Pulse Bursts via a Potassium Gadolinium Tungstate Raman Laser

Aleksandr Tarasov * and **Hong Chu**

Laseroptek, 204 Hyundai I Valley, 31 Galmachi-ro, 244 Beon-gil, Jungwon-gu, Seongnam-si 13212, Gyeonggi-do, Republic of Korea; hongchu@laseroptek.com
* Correspondence: aatarasov@laseroptek.com

Abstract: In this study, pulse bursts at 559, 589, and 621 nm, with a record energy of ~10 J, are generated using a KGW Raman laser with an external resonator, while pumping at 532 nm. The pulse bursts have a 10 ms duration, and consist of 78 subpulses with a duration of <10 ns, at 8 kHz. The maximum energy of the bursts is restricted only by the characteristics of the Nd: YAG laser used as the 532 nm pump source, and can be increased.

Keywords: Raman laser; solid-state laser; pulse-burst laser; KGW crystal; stimulated Raman scattering

Citation: Tarasov, A.; Chu, H. Wavelength Conversion of Multi-Joule Energy 532 nm Pulse Bursts via a Potassium Gadolinium Tungstate Raman Laser. *Appl. Sci.* **2023**, *13*, 10195. https://doi.org/10.3390/app131810195

Academic Editor: Humberto Cabrera

Received: 4 August 2023
Revised: 6 September 2023
Accepted: 8 September 2023
Published: 11 September 2023

1. Introduction

Lasers that generate in pulse-burst mode can be used in high-speed photography, gas flow and plasma diagnostics, dermatology, cosmetic medicine, etc. [1–3]. According to a recent review [1], currently, most of these systems are based on 1064 nm Nd: YAG lasers. Wavelength diversification considerably increases the capabilities of systems. Many different methods of 1064 nm wavelength conversion, especially into the visible spectral range, have been investigated for use in pulse-burst-generation mode, the main examples being harmonic generation, optical parametric generation, and the pumping of dye lasers. Interestingly, wavelength conversion using stimulated Raman scattering applied to pulse-burst lasers has not been scrutinized previously. We found only two publications in which Raman conversion was produced in pulse-burst mode in the NIR range [4,5]. To the best of our knowledge, there are no publications on the Raman conversion of multi-joule energy pulse-burst lasers into the visible range.

For crystalline Raman lasers, most of the studies from the last decade [6–9] have focused on increasing the average power of lasers operating in continuous-wave (CW) mode, or generating pulses with a high repetition rate (~10^5 Hz) and relatively low (<1 mJ) energy. In these cases, the Raman gain coefficient required for the efficient conversion of the pump radiation into Stokes components is achieved only if the pump radiation is concentrated in a spot of relatively small (<0.2 mm) size. Accordingly, with an increase in the average pump power, a significant temperature gradient is created in the Raman crystal, leading to strong thermo-optical distortions. These distortions comprise the main physical factor limiting an increase in the average power of such lasers. Such an increase can only be achieved using diamond crystals, which have a ~1000 times higher thermal conductivity than other known Raman crystals [10]; however, their use in practice is limited, due to the high cost of diamonds, and the small size of the available crystals.

Operating Raman lasers in pulse-burst mode allows another approach to Raman laser energy and power scaling. If the power of individual pulses (subpulses) in the burst is sufficient for efficient Raman conversion without tight focusing, then the temperature gradient and corresponding thermo-optical distortions in the Raman crystal can be considerably reduced. Considering, for simplicity, the generating volume as a cylinder with radial heat flow, and using a formula [11] for the thermal lens dioptric power $\mathbf{f^{-1}}$:

$$\mathbf{f^{-1} \sim P/d^2}$$

(here, **P** is a heat power, dissipated within a cylinder of diameter **d**), one can estimate that an increase in the generating spot diameter from 0.2 mm to 4 mm should result in a ~400-times reduction in the thermal lens power in the Raman crystal. This would allow a significant increase in the energy and average power of a Raman laser, even when using standard Raman crystals, such as potassium gadolinium tungstate (KGW). It should be noted that the largest burst energy previously realized in Raman lasers was 1.6 J at 1180 nm, which was obtained using a BaWO4 crystal pumped via a 2.5 ms burst of 50 Q-switched subpulses at 1062 nm, with a burst energy of 19 J from a Nd: GGG laser [4].

In this paper, we study the generation of high-energy bursts in the visible spectral range, using an external resonator Raman laser with a KGW crystal. The practical goal is to create an all-solid-state yellow–orange (585–595 nm) laser with an energy of at least 8 J, irradiated with 10^{-2}–10^{-3} s bursts at a ~1 Hz repetition rate, for application in dermatology and cosmetic medicine. So far, such high-level energy characteristics have only been achievable in flash-lamp-pumped organic dye lasers (model "Vbeam", manufactured by Candela. The characteristics of this laser can be found at https://candelamedical.com/products/vbeam-perfecta, accessed on 1 March 2023). The high efficacy of pulsed dye yellow laser irradiation for the medical treatment of different dermatologic diseases has been proved many times (see, for example, [12,13]). Unfortunately, pulsed dye lasers have multiple inherent disadvantages; one of the most important is organic dye's short operational time of fewer than 10^5 pulses.

There are two main ways to obtain yellow–orange radiation from KGW Raman lasers pumped via Nd: YAG lasers. The first is the Raman conversion of 1064 nm radiation into the first Stokes order at 1178 nm, with subsequent second-harmonic generation (SHG): 1178 nm → 589 nm. The most suitable crystal for SHG at this wavelength is LBO. Unfortunately, the angular acceptance of this crystal is relatively small, so a good SHG efficiency can be obtained only for radiation with a high beam quality. This method was used in [6–9], where Raman lasers with a small pump spot size were operated at low-order transversal modes. However, in our approach, increasing the pumping beam spot size led to a considerable increase in the Raman laser beam angular divergence, which results in a low SHG efficiency. For this reason, we selected the second approach, where 532 nm radiation is generated first via 1064 nm SHG in a KTP crystal, allowing a high SHG efficiency. Then, a KGW Raman laser is used to selectively generate the second Stokes component at 589 nm under 532 nm pumping. Raman laser efficiency, in general, does not depend on the angular characteristics of the pumping radiation, so we expect a good overall efficiency in the wavelength conversion.

In contrast to cavity-less Raman conversion, the use of mirrors with appropriate spectral characteristics in a Raman laser makes it possible to control the generation threshold, and ensure the selective generation of the required individual Stokes components. This possibility was discussed and qualitatively demonstrated in previously published works (for example, see [14], and the review in [15]), but no exact quantitative requirements for mirrors and pumping conditions were formulated, especially for a high pump power density. In our work, we determine the values of the optimal spectral transmittance of the output mirrors, and realize selective generation at 589 nm, 559 nm, and 621 nm, with a high efficiency, and an energy of 8–13 J in 10 ms bursts.

It should be mentioned that some preliminary results of our investigation have been reported at Optica Advanced Photonics Congress 2022 in Barcelona, Spain. The technical digests of the presentation have already been published in [16]. Here, we do not repeat any information related to the preliminary investigation. Only new, improved results are included and discussed in this manuscript.

2. Experimental Hardware

A block scheme of the experimental setup is shown in Figure 1.

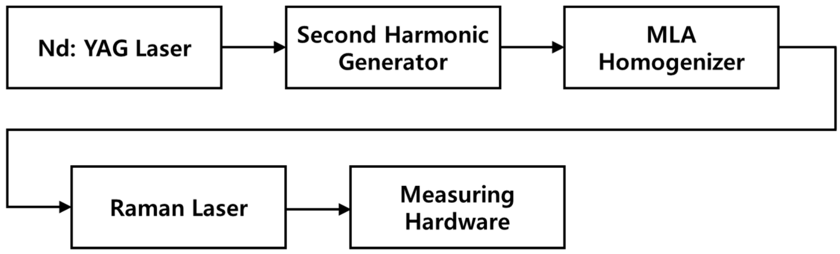

Figure 1. The experimental setup.

To study wavelength conversion in a KGW Raman laser, we arranged a relatively simple high-energy Nd: YAG laser that could operate in pulse-burst mode (PB mode), as well as in single-pulse mode (SP mode), using two different power supplies. It should be mentioned that operation in SP mode allows us to simplify and accelerate the laser alignment procedure, optimize the Raman laser parameters, etc. The Nd: YAG laser included a flash-lamp-pumped electro-optically Q-switched multimode oscillator, followed by a single-stage amplifier. The laser's Pockels cell driver had a variable Q-switching rate up to 10 kHz, to produce pulse bursts within a 10 ms flash lamp pump pulse, as well as to produce single pulses in combination with a 200 µs flash lamp pulse when operated in SP mode. The laser's characteristics are shown in Table 1.

Table 1. The characteristics of the Nd: YAG laser.

Pulse-Burst Mode	
Burst repetition rate	1–1.5 Hz
Subpulse repetition rate within the burst	5–10 kHz
Burst duration	10 ms
Subpulse duration	12–15 ns
Maximum burst energy	45 J
Single-Pulse Mode	
Maximum pulse repetition rate	10 Hz
Minimum pulse duration	6 ns
Maximum pulse energy	0.8 J

SHG was obtained using a 5 mm length KTP crystal. The SHG efficiency in PB mode reached 50%, and the maximum burst energy at 532 nm was 23 J. The minimum subpulse duration here was 10 ns. In SP mode, the maximum pulse energy was 0.4 J, and the minimum pulse duration was 5 ns.

The optical scheme of the external-cavity Raman laser is shown in Figure 2. The laser included a 7 × 7 × 50 mm "N_P"-cut KGW crystal from Eksma Optics, with two flat mirrors: a pump and an output. The pump mirror had 93–95% transmission at 532 nm and 99.5% reflection within 550–670 nm. The output mirror had 99.5% reflection at 532 nm, to produce double-pass pumping. The reflection coefficients of the output mirrors at other wavelengths were varied, to determine the optimum values to selectively generate the first, second, or third Stokes order. Both mirrors were placed close to the ends of the KGW crystal, so the resonator length was 52–54 mm.

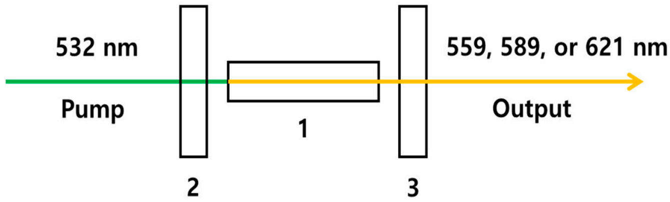

Figure 2. The optical scheme of the Raman laser. 1, the KGW crystal; 2, the pump mirror; 3, the output mirror.

A pumping radiation of 532 nm was transmitted through a single microlens array (MLA) homogenizer, and focused into a KGW crystal via a condenser lens, producing a sharp 4.1 × 4.1 mm rectangular cross-section channel along the crystal. The polarization of the 532 nm radiation was set to be parallel to the axis N_m, to obtain a Stokes shift of 901 cm^{-1}.

The laser energy in SP mode at all wavelengths was measured with a J-50-YAG pyroelectric detector from Coherent and, in PB mode, with a 30(150) A-LP2-18 thermophile sensor from Ophir. The subpulse duration was determined using a UPD-50-UD photodetector from Alphalas (50 ps rise time), and an Infinium DSO80804B digital oscilloscope with an 8 GHz bandwidth. The time dependence of the subpulses in PB mode was recorded using DET 36 photodetectors from Thorlabs, and a Tektronix 5204B oscilloscope. The spectrum of Raman laser generation was registered using a Flame–S–VIS-NIR-EO miniature spectrometer from Ocean Insight.

3. Results and Discussion

3.1. Conditions Required for the Selective Generation of Stokes Orders with Maximum Conversion Efficiency

The characteristics of a pulse-burst Raman laser significantly depend on the characteristics of the pumping radiation, and the spectral reflectance of the output mirrors. The optimum values of the pump subpulse power density, $\mathbf{p_{532}}$, and the reflection coefficients, $\mathbf{R_\lambda}$, of the output mirrors at the wavelengths of the first, second, and third Stokes order were determined during operation in SP mode, and used for operation in BP mode.

To obtain the high Raman laser energy $\mathbf{E_{RAM}}$, and the energy efficiency $\boldsymbol{\eta}$ ($\boldsymbol{\eta}$ = $\mathbf{E_{RAM}}/\mathbf{E_{532}}$, $\mathbf{E_{532}}$ is the energy of the 532 nm pump radiation), we produced an optimization of the Raman laser output mirrors for $\mathbf{p_{532}} \geq 100$ MW/cm^2. The maximum level of $\mathbf{p_{532}}$ was always restricted by the appearance of the higher (unwanted) Stokes order. Table 2 indicates the values of $\mathbf{p_{532}}$ (max), measured when the higher Raman order intensity reached 5% of the intensity of the required order (an estimation was made using the spectral line intensity ratio), and $\boldsymbol{\eta}$ for three combinations of mirror reflection coefficients, which were used in the experiment to optimize the generation of the second Stokes order (589 nm).

Table 2. The optimum parameters for the selective generation of the second Stokes order.

	Mirror Reflection Coefficients, R_λ	p_{532} (max)	η %
1	$\mathbf{R_{559}}$ = 99.5%, $\mathbf{R_{589}}$ = 1.5%, $\mathbf{R_{621}}$ = 0.6%	~200 MW/cm^2	58
2	$\mathbf{R_{559}}$ = 99.5%, $\mathbf{R_{589}}$ = 10.5%, $\mathbf{R_{621}}$ = 0.35%	~260 MW/cm^2	60
3	$\mathbf{R_{559}}$ = 99.5%, $\mathbf{R_{589}}$ < 0.3%, $\mathbf{R_{621}}$ < 0.1%	~320 MW/cm^2	62

Similar results were obtained for the first (559 nm) and the third (621 nm) Stokes orders:

- For 559 nm: $\mathbf{R_{559}}$ = 2%, $\mathbf{R_{589}}$ < 1%, $\mathbf{p_{532}}$ (max) ~200 MW/cm^2, $\boldsymbol{\eta}$ = 63%;
- For 621 nm: $\mathbf{R_{559}}$ = 99.5%, $\mathbf{R_{589}}$ = 99.2%, $\mathbf{R_{621}}$ = 1.8%, $\mathbf{R_{654}}$ = 1.9%, $\mathbf{p_{532}}$ (max) ~300 MW/cm^2, $\boldsymbol{\eta}$ = 50%.

One can see that the best results were obtained using output mirrors with characteristics similar to long-pass filters with a cut-off wavelength that corresponds to the wavelength of the required Raman order. The reflection coefficient at the required wavelength does not significantly affect the characteristics of the Raman laser. However, the reflection coefficient at the wavelength of the next Stokes component should be minimal, to increase the threshold of the unwanted order. All these results are a consequence of the large Raman gain in our experimental conditions. A simple calculation shows that, using a double-pass pumping scheme with a 4.1 × 4.1 mm pumping spot, and 50 mm length crystal (the KGW steady-state gain is 11.8 cm/GW [6]) in SP mode, we can obtain a gain increment G > 25, allowing the efficient conversion of pump radiation into Stokes radiation [17], even in a cavity-less configuration, at $\mathbf{E_{532}}$ ~ 0.2 J, which is two times less than the maximum energy of our 532 nm source.

3.2. Energy Characteristics of Pulse-Burst Generation

The best values for the energy characteristics of the Raman laser in PB mode were obtained when the Q-switching rate and, correspondingly, the subpulse repetition rate, were 7.6–8 kHz. We obtained 75–78 subpulses in the burst (see Figure 3).

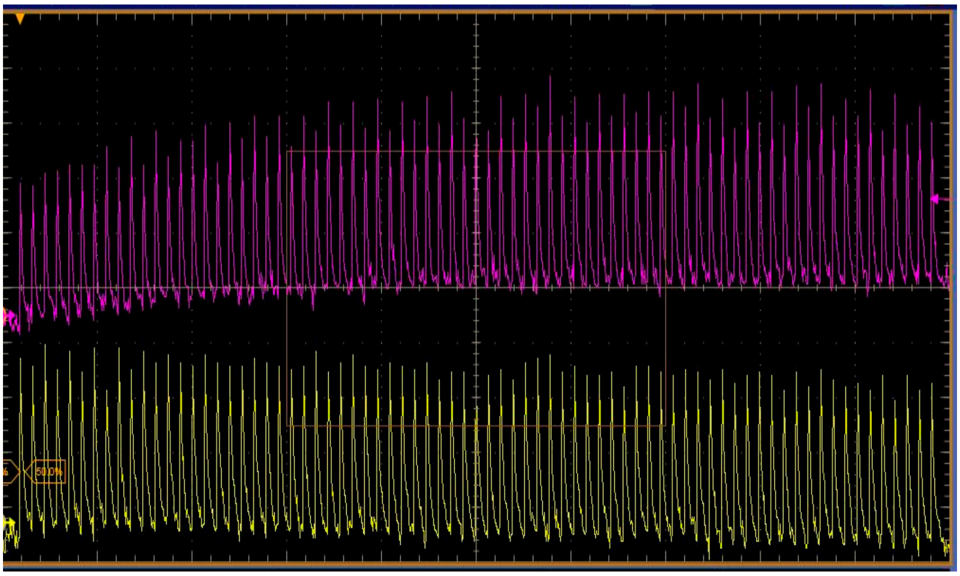

Figure 3. The oscillograms of the burst pulse at an 8 kHz Q-switching rate: pink, 532 nm pump radiation; yellow, 589 nm Raman radiation. The frame width is 10 ms.

The maximum electric pump energy applied to flash lamps operating in PB mode exceeds 1500 J, so the average pump power, even at 1 Hz, can exceed 1.5 kW. It caused a considerable thermal birefringence in the Nd: YAG laser rods, and the reduction in Nd: YAG laser energy after the start. Correspondingly, the burst energies at 532 nm and all Stokes wavelengths also decreased. The temporal decrease in the burst energy at 532 nm and 589 nm is shown in Figure 4.

At the same time, we can see that the efficiency of 589 nm generation remains practically unchanged after more than 2 min of laser operation. This means that $\mathbf{E_{589}}$ reduces only in proportion to the reduction in $\mathbf{E_{532}}$, indicating that, for our pumping spot size, the thermo-optical distortions that are created in the KGW crystal during Raman laser generation are actually small, and do not exert a notable additional influence on the Raman laser energy.

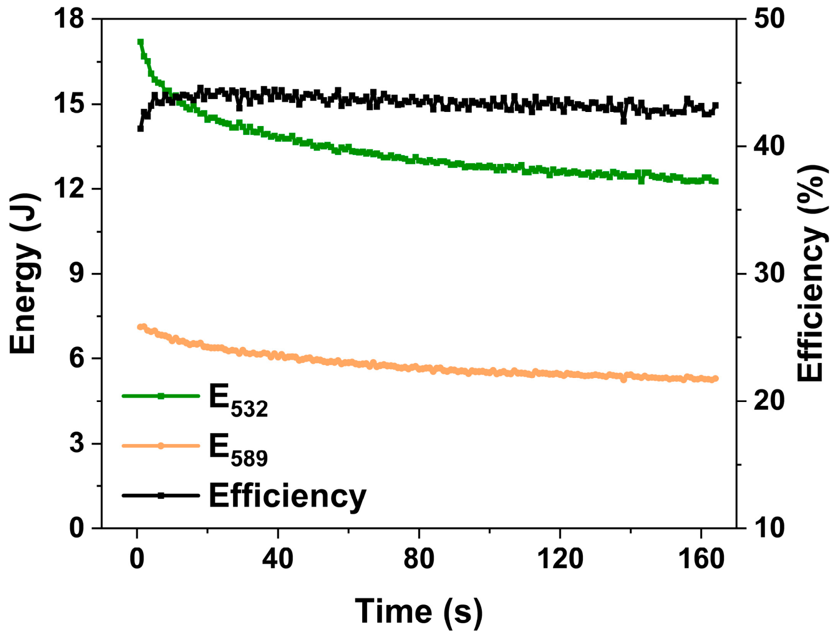

Figure 4. The temporal behavior of the laser burst energy and Raman laser efficiency. The burst repetition rate is 1 Hz. The electrical pump energy applied to Nd: YAG laser flash lamps is 1250 J, which is ~80% of the maximum available pump energy.

Figure 5 shows the dependence of the burst energies of the first, second, and third Stokes orders on a 532 nm pump energy. The energy values indicated here were measured at the fifth burst after the start.

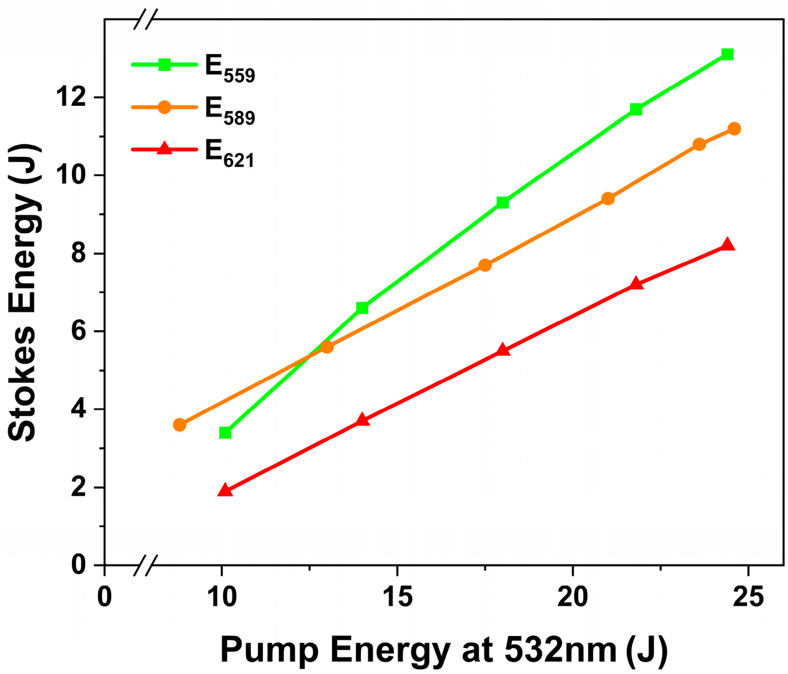

Figure 5. The dependence of the Raman laser burst energy on 532 nm pump burst energy for the generation of 559 nm, 589 nm, and 621 nm Stokes orders. The 589 nm order was generated using output mirror 1 (Table 2). The burst repetition rate is 1 Hz.

At the maximum 532 nm pump energy $\mathbf{E}_{532}$ = 23 J, we obtained a burst energy $\mathbf{E}_{559}$ = 13 J at 559 nm, $\mathbf{E}_{589}$ = 11.6 J at 589 nm, and $\mathbf{E}_{621}$ = 8 J at 621 nm. This is the first time that such a level of energy in Raman lasers for the visible spectral range has been realized. The maximum energy achieved here at 559 nm is eight times higher than that previously reported in [4] for 1180 nm. The maximum energy efficiencies, **η**, here, are 56%, 50%, and 35% for 559 nm, 589 nm, and 621 nm, respectively.

The increase in the Nd: YAG laser's burst repetition rate from 1 Hz to 1.5 Hz was followed by an additional decrease in burst energies at all wavelengths at the given electric pump level. In Figure 6, we combine the burst energy data obtained at 1.0 and 1.5 Hz. One can see that all the dots lie on the same straight line. This means that the Raman laser efficiency does not reduce when the burst repetition rate increases from 1 Hz to 1.5 Hz. At 1.5 Hz, thermal distortions, of course, are larger than at 1 Hz, but this does not cause a reduction in efficiency. In our opinion, this also confirms the conclusion, which was expressed earlier, that thermo-optical distortions in a KGW crystal under our operational conditions do not cause a notable deterioration in the laser energy. Thus, we can expect to obtain larger output energies and average powers from a KGW Raman laser in PB mode by improving the characteristics of Nd: YAG lasers.

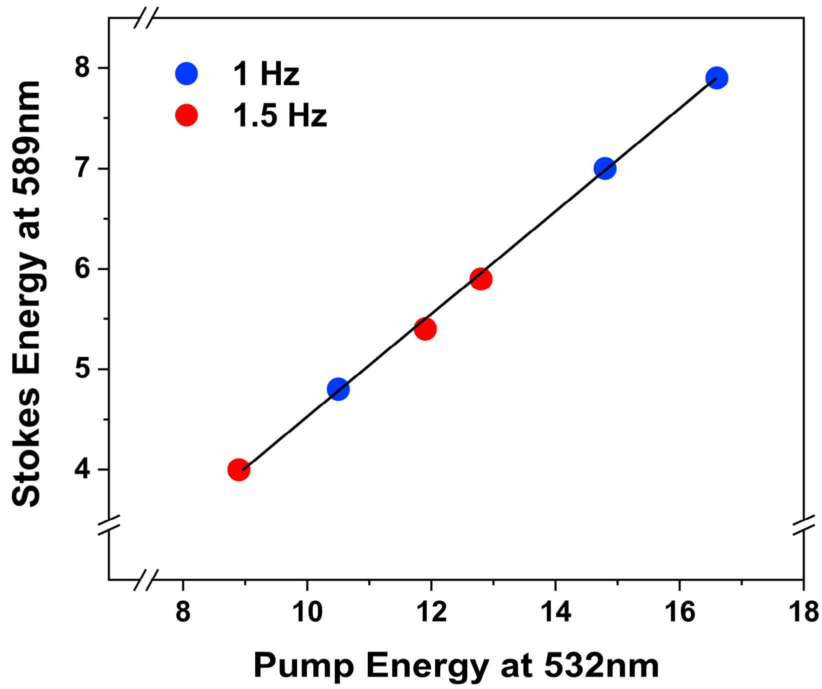

Figure 6. $\mathbf{E_{589}}$ versus $\mathbf{E_{532}}$ for the burst repetition rates of 1 and 1.5 Hz.

The efficiency of the Raman laser generation achieved in PB mode was 12–20% lower than that obtained in SP mode at an equal pump energy density (considering the average energy density of individual subpulses in a 532 nm burst). The lower values of **η** here can be explained by the fact that, when operating in BP mode, the pulse duration of 532 nm radiation in our laser is approximately 1.5–1.8 times longer than in SP mode, so, at an equal pump energy density, the power density, $\mathbf{p_{532}}$, is correspondingly lower, resulting in lower **η**.

Angular distribution of Raman laser burst energy, measured at 1 Hz for $\mathbf{E_{589}}$ = 10 J, is shown in Figure 7. We see that 50% of energy is concentrated within 12 mrad. Considering this value as a beam angular divergence, and the pumping spot size 4.1 mm as a beam waist diameter, we can estimate that the beam parameter product BPP = 12 mm × 4.1 mm × mrad, and the beam quality parameter M^2 = 65.

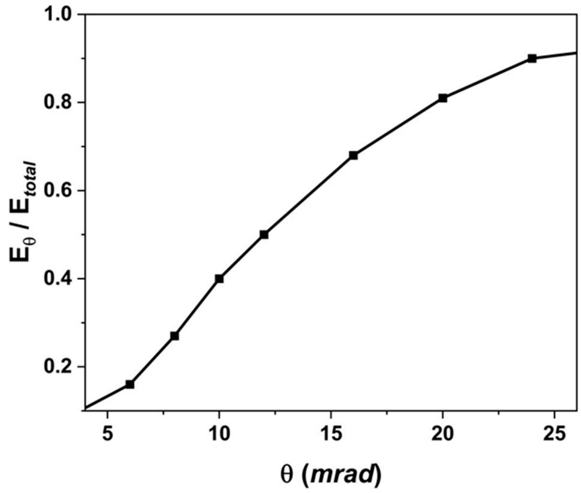

Figure 7. The Raman laser energy angular distribution. Here, $\mathbf{E_\theta}$ is the energy, irradiated at angle θ, and $\mathbf{E_{total}}$ is the total energy of the Raman laser.

4. Conclusions

In this work, we generated, for the first time, multi-joule pulse bursts with a millisecond duration at three different Stokes orders in the visible spectral range, using a crystalline Raman laser with standard affordable KGW crystals. A record-breaking level of burst energy, exceeding 10 J at 559 nm and 589 nm, was achieved at the three Stokes orders. No essential deterioration in the Raman laser energy efficiency was found at an average pump power exceeding 20 W.

We speculate that operating in PB mode, using standard KGW crystals and an increased pump spot size, will allow the achievement of a Raman laser average power that was previously only possible with diamond crystals.

We must emphasize that the output energy and average power of the Raman laser in our work were restricted by the characteristics of the Nd: YAG laser used for pumping. It is expected that larger Raman laser burst energies and average powers could be obtained with a more powerful pumping source.

This work represents an important practical result, as we consider it to be the first time that these characteristics, which could previously only be achieved using dermatological pulsed dye lasers, have been realized in all-solid-state lasers.

Author Contributions: A.T. and H.C. contributed equally to this work. All authors have read and agreed to the published version of the manuscript.

Funding: This work was supported by the Technological Innovation R&D Program (S3272695), funded by the Ministry of SMEs and Startups (MSS, Korea).

Data Availability Statement: The data underlying the results presented at this paper are not publicly available at this time but may be obtained from the authors upon reasonable request.

Acknowledgments: The authors thank Park Kyu Tai for his help with preparing the paper's figures.

Conflicts of Interest: The authors declare no conflict of interest.

References

1. Slipchenko, M.; Meyer, T.; Roy, S. Advances in burst-mode laser diagnostics for reacting and nonreacting flows. *Proc. Combust. Inst.* **2021**, *38*, 1533–1560. [CrossRef]
2. Jiang, N.; Webster, M.; Lempert, W. Advances in generation of high-repetition-rate burst mode laser output. *Appl. Opt.* **2009**, *48*, B23–B31. [CrossRef] [PubMed]
3. Husain, Z.; Alster, T. The role of lasers and intense pulsed light technology in dermatology. *Clin. Cosmet. Investig. Dermatol.* **2016**, *9*, 29–40. [PubMed]

4. Basiev, T.; Danileiko, Y.; Doroshenko, M.; Osiko, V.; Fedin, A.; Gavrilov, A.; Smetanin, S. Powerful BaWO4 Raman laser pumped by a self-phase-conjugated Nd: YAG and Nd: GGG lasers. In Proceedings of the Advanced Solid-State Photonics 2004, Santa Fe, NM, USA, 1–4 February 2004; OSA: Washington, DC, USA, 2004. Paper TuB11.
5. Chulkov, R.; Lisinetskii, V.; Lux, O.; Rhee, H.; Shrader, S.; Eichler, H.; Orlovich, V. Thermal aberrations and high power frequency conversion in a barium nitrate Raman laser. *Appl. Phys. B* **2012**, *106*, 867–875. [CrossRef]
6. Pask, H.; Piper, J. Raman Lasers. In *Handbook of Solid-State Lasers*; Denker, B., Shklovsky, E., Eds.; Woodhead Publishing Limited: Cambridge, UK, 2013; pp. 493–524.
7. Sarang, S.; Richardson, M. Power scaling of CW crystalline OPOs and Raman lasers. *Photonics* **2021**, *8*, 565. [CrossRef]
8. Hsiao, J.; Hwang, Y.; Lee, C.; Yu, Y.; Tsou, C.; Liang, H.; Chen, Y. Powerful Q-switched Raman laser at 589 nm with a repetition rate between 200 and 500 kHz. *Opt. Lett.* **2021**, *46*, 2063–2066. [CrossRef] [PubMed]
9. McKay, A.; Kitzler, O.; Mildren, R. High power tungstate-crystal Raman laser operating in the strong thermal lensing regime. *Opt. Express* **2014**, *22*, 707–715. [CrossRef] [PubMed]
10. Williams, R.; Kitzler, O.; Bai, Z.; Sarang, S.; Jasbeer, H.; McKay, A.; Antipov, S.; Sabella, A.; Lux, O.; Spence, D.; et al. High power diamond Raman lasers. *IEEE J. Sel. Top. Quantum Electron.* **2018**, *24*, 1602214. [CrossRef]
11. Koechner, W. *Solid-State Laser Engineering*, 4th ed.; Springer: Berlin/Heidelberg, Germany, 1996; p. 402. ISBN 3-540-60237-2.
12. Galeskas, K.; Ross, E.; Uebelhoer, N. A pulsed dye laser with a 10-mm beam diameter and pigmented lesion window for purpura-free photorejuvenation. *Dermatol. Surg.* **2008**, *34*, 308–313.
13. Halachmi, S.; Israeli, H.; Ben-Amitai, D.; Lapidoth, M. Treatment of the skin manifestations of hereditary hemorrhagic telangiectasia with pulsed dye laser. *Lasers Med. Sci.* **2014**, *29*, 321–324. [CrossRef] [PubMed]
14. Lisinetskii, V.; Grabtchikov, A.; Khodasevich, I.; Eichler, H.; Orlovich, V. Efficient high energy 1st, 2nd or 3rd Stokes Raman generation in IR region. *Opt. Commun.* **2007**, *272*, 509–513. [CrossRef]
15. Pask, H.; Dekker, P.; Mildren, R.; Spence, D.; Piper, J. Wavelength-versatile visible and UV sources based on crystalline Raman lasers. *Prog. Quant. Electron.* **2008**, *32*, 121–158. [CrossRef]
16. Tarasov, A.; Chu, H. Multijoule yellow light pulse burst generation by KGW Raman laser. In Proceedings of the Technical Digest Series, Optica Advanced Photonics Congress, Barcelona, Spain, 11–15 December 2022. Optica Publishing Group, 2022; Paper AW4A.2.
17. Spence, D. Spectral effects of stimulated Raman scattering in crystals. *Prog. Quant. Electron.* **2017**, *51*, 1–45. [CrossRef]